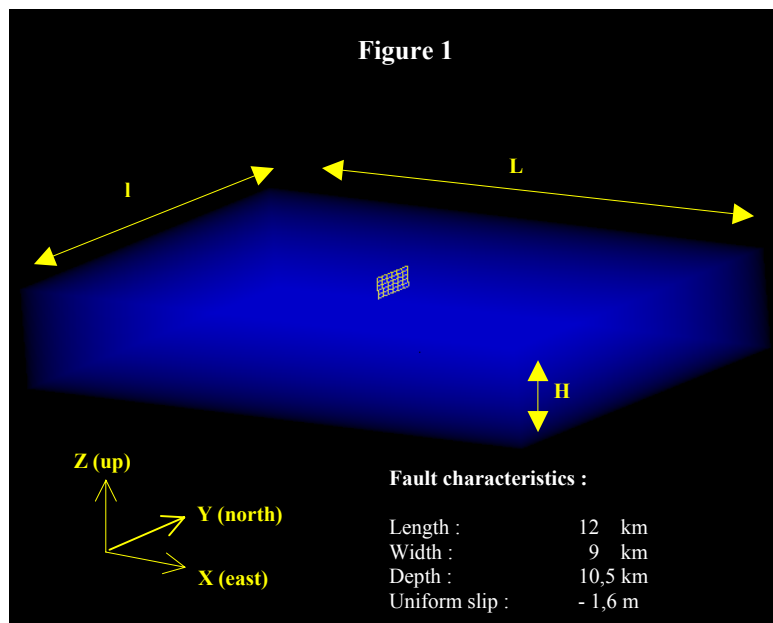


# Finite-element modelling of coseismic crustal deformation : simple tests to study the convergence and the capabilities of the TEKTON software package

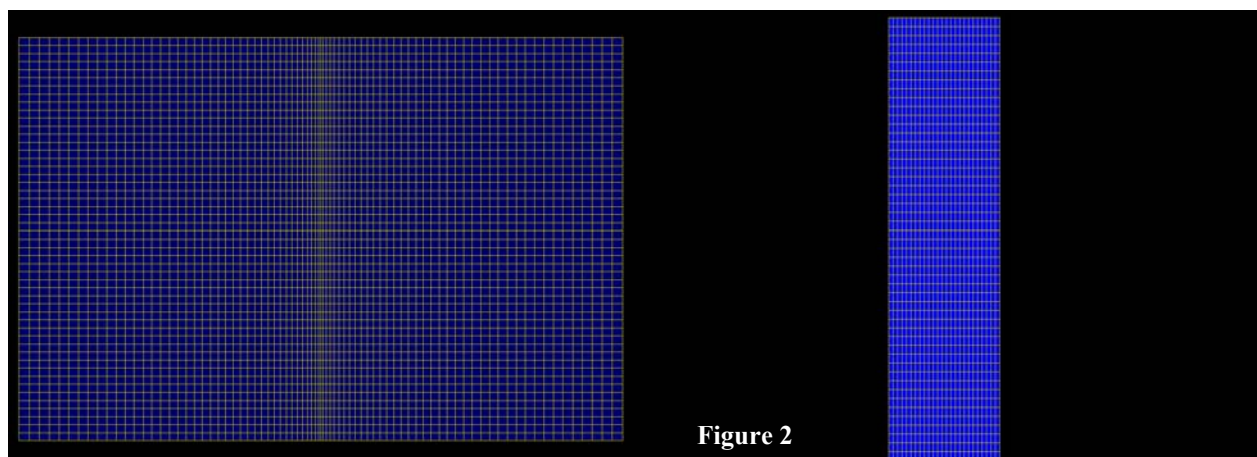
Loïc Dubois, Kurt L. Feigl, Dimitri Komatitsch

In June 2000, two large earthquakes of magnitude 6.6 occurred in the South Iceland Seismic Zone. To model the crustal deformation associated with these events, we are in the process of developing a 3D finite-element model for the TEKTON software package. We perform comparative tests with the analytic solution of Okada (1985) to validate this model. The reference solution of Okada (1985) was numerically computed based on the RNGCHN software package (Feigl & Dupré 1999).

The validation model is a right-lateral vertical N-S strike uniform slip fault in a homogenous elastic half-space. We need ten parameters to define this fault : the three coordinates of Okada's origin easting  $E$ , northing  $N$  and depth  $d$ , strike  $\alpha$  ( $0^\circ$ ), dip  $\delta$  ( $90^\circ$ ), length  $L_f$ , width  $W_f$  and the three components of the slip vector (here there is only one in the  $Y$  direction). The surface projection of the fault is located in the centre of our model (figure 1). We assume that the five buried boundaries are fixed. The surface has a free boundary condition.



A few initial tests enabled us to define a finite-element mesh adapted to our problem. It is a hexahedral mesh that respects the two edges of the fault. The grid is regular in the  $Y$  (North) and  $Z$  (up) directions. In the  $X$  (East) direction, the size of the elements increases with the distance to the fault (figure 2).



We have chosen the TEKTON formulation because it allows “split nodes” as described by Melosh & Raefsky (1981). Accordingly, we specify 1.6 m of slip at each node in the rupture patch. At these split nodes, the displacement is discontinuous with 0.8 m on one side of the fault and 0.8 on the other, in the opposite direction.

## I. CPU Time

After running Tekton on models with a different number of elements, we find a relation between CPU time and number of both elements and nodes (figure 3). Basically the CPU time seems to be linearly linked to the memory used (figure 4). The computer is a 2.4 GHz PC with 1Gb RAM running Linux Red Hat 7.3 and the Intel Fortran compiler “ifc”. We have recompiled for each model to use the exact memory needed by TEKTON to run it.

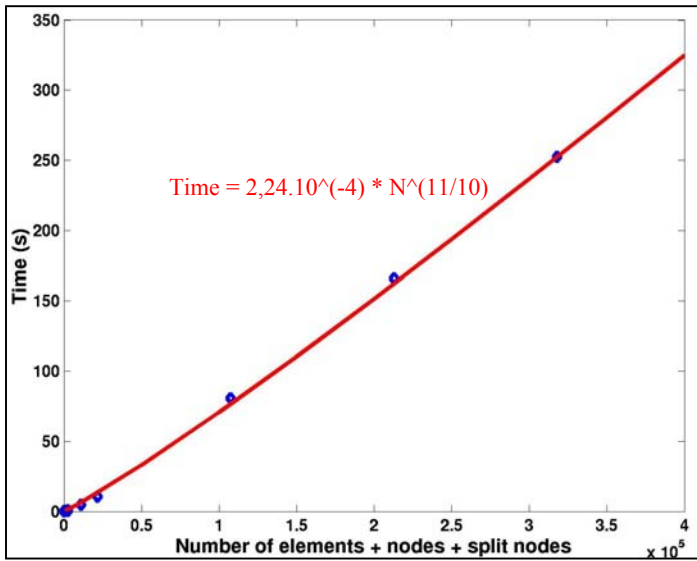


Figure 3 – Calculation time CPU as a function of total number of elements, nodes and split nodes

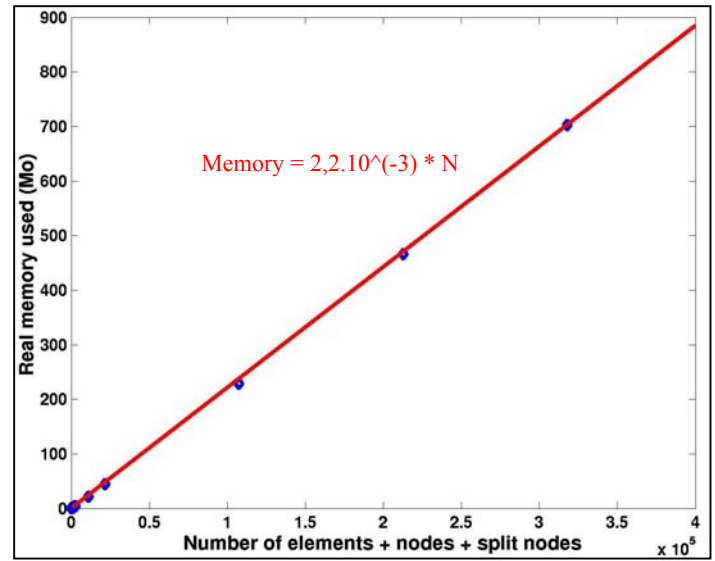


Figure 4 – Real memory used as a function of total number of elements, nodes and split nodes

## II. Overall convergence

The method used consists in finding :

(1) The displacements computed by RNGCHN at observation points of a grid, which defines our study area at the free surface. This grid is centred on the fault and its dimensions are 180 km long and 100 km wide. We take these values as a reference.

(2) The nodal displacements for a given number of elements by running TEKTON on a model with  $L = 300$  km,  $l = 204$  km and  $H = 54$  km (see figure 1 above).

(3) The displacements at the observation points on the same surface grid based upon a first-order interpolation of the Tekton values.

When we compute the absolute value of the error between values (2) and (3) found at the observation points. This calculation is performed in each direction ( $err(U_x)$ ,  $err(U_y)$ ,  $err(U_z)$ ) and for the norm of displacement vector ( $err(U)$ ). Then the sum over all points and the sum of the L1 norms ( $err(U_x) + err(U_y) + err(U_z)$ ) measure the accuracy of the model.

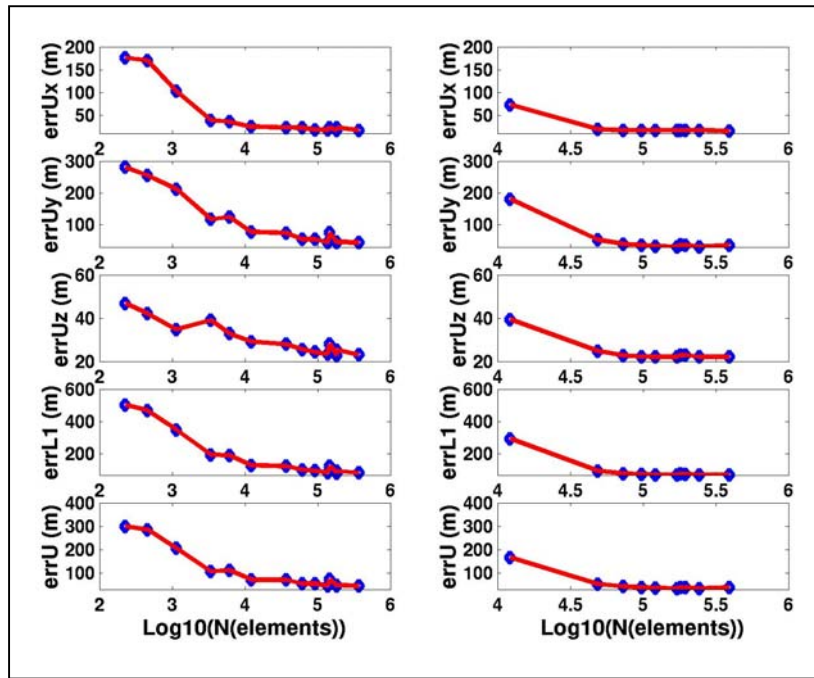


Figure 5 – Convergence (regular mesh vs. mesh which varies along X only)

Figure 5 shows a test of convergence. Here the regular mesh corresponds to a case with elements of the same size. The mesh, which varies along X only, is described above. The figure illustrates that the second mesh is well adapted to the large variations in displacement near the fault because of its density.

Figure 5 also points out that the problem converges for about 60K elements. Basically it ensures us that a model with 100K elements gives accurate results.

### III. Boundary effects

To illustrate the effect of boundary conditions, we study two models :

Model 1 :       $N_x = 50$  elements       $L = 300$  km       $\Delta x : 0.5 \rightarrow 10.3$  km  
                   $N_y = 68$  elements       $l = 204$  km       $\Delta y = 3$  km  
                   $N_z = 36$  elements       $H = 54$  km       $\Delta z = 1.5$  km

Model 2 :       $N_x = 60$  elements       $L = 600$  km       $\Delta x : 0.8 \rightarrow 17.3$  km  
                   $N_y = 100$  elements       $l = 300$  km       $\Delta y = 3$  km  
                   $N_z = 60$  elements       $H = 90$  km       $\Delta z = 1.5$  km

Different calculations were performed on each model. We take several boundary conditions (X, Y faces and lower Z face can be fixed or free) and two kinds of boundary elements (infinite or finite). Figure 6 summarizes the overall error in L1 norm, the overall errors in each direction and the overall error for the displacement vector norm.

	X sides fixed	Y sides fixed	Zmin side fixed	Infinite element	Error on Ux (in m)	Error on Uy (in m)	Error on Uz (in m)	Error in L1 norm (in m)	Error on   U   (in m)
Model 1	X	X	X		14.4	28.8	17.5	60.7	29.8
	X	X	X	X	14.6	29.7	18.0	62.3	30.5
	X	X			7.4	10.8	19.1	37.3	10.1
	X		X		12.3	18.4	16.9	47.5	21.4
		X	X		13.4	28.2	17.5	59.1	28.7
Model 2	X	X	X		8.4	15.9	11.5	35.8	16.0
	X	X			7.5	9.1	10.0	26.6	9.2
	X		X		7.6	11.7	11.3	30.6	11.7
		X	X		8.4	15.9	11.5	35.8	16.0

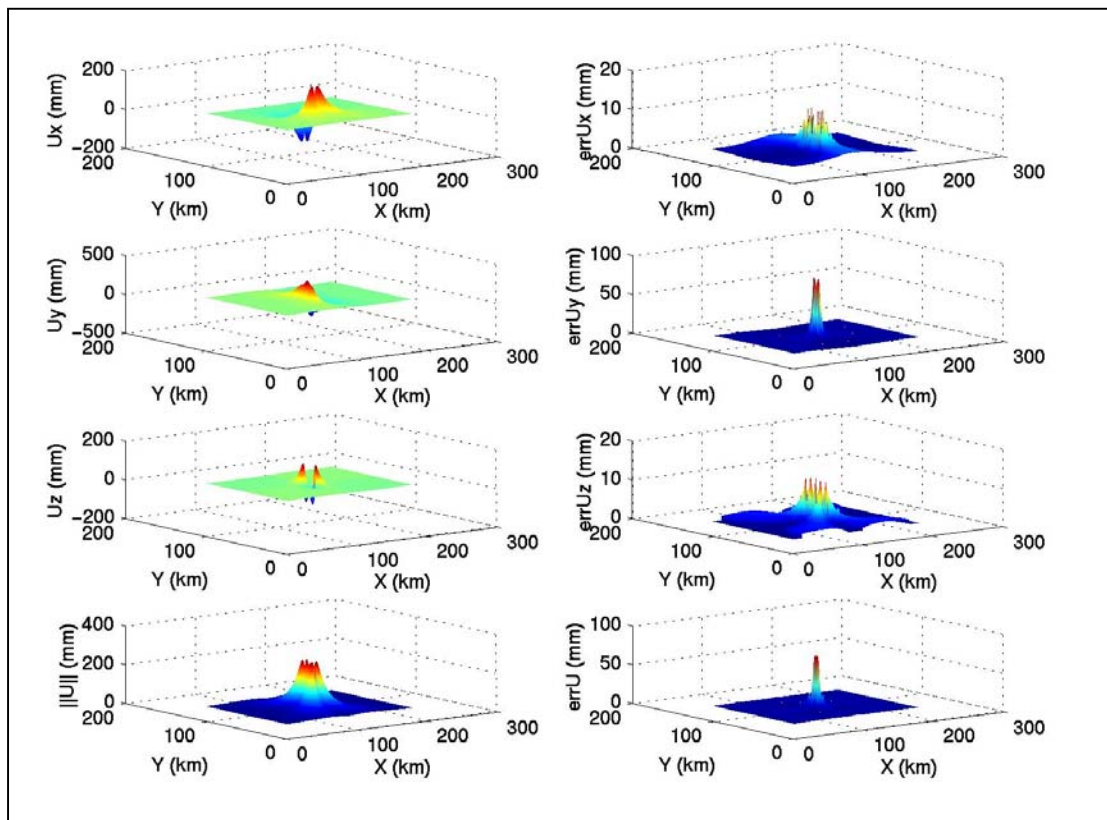
**Figure 6** – Table of errors with different element sizes and boundary conditions.

Figure 6 points out the large sensitivity to the boundary conditions on the Z face. It also shows a sensitivity on the Y faces. However, the model is not so sensitive to the conditions along the X faces. The first two lines illustrate that infinite elements are not particularly useful in our case.

In the second model, the sensitivity is negligible on the X faces. On the other hand, the results are still sensitive to the boundary conditions on the Y faces and even more on the Z face.

#### IV. Local convergence

For the first model, figure 7 gives an example of surface displacements on the study area (180km x 100km) given by Okada (1985) and a representation of the error of our model. The left figures show the values of the displacement in the three directions. The fourth figure is the norm of the displacement vector. The right figures are the representation of the error between the Okada and TEKTON values for the three directions and the norm of the displacement vector.



**Figure 7** – Okada (1985) displacements (left) and Model vs. Okada errors in the study area (right)

In all the tests there is always the same peak of errors in the vicinity of the fault. This peak does not seem to be very sensitive to the boundary conditions. However, when these tests are compared to similar tests with an 18 km deep fault instead of 10.5 km (figure 8 to 12), a close-up on the fault area illustrates that TEKTON does not manage to follow the large variations of the displacements. Therefore this peak could be the result of poor convergence in the vicinity of the fault.

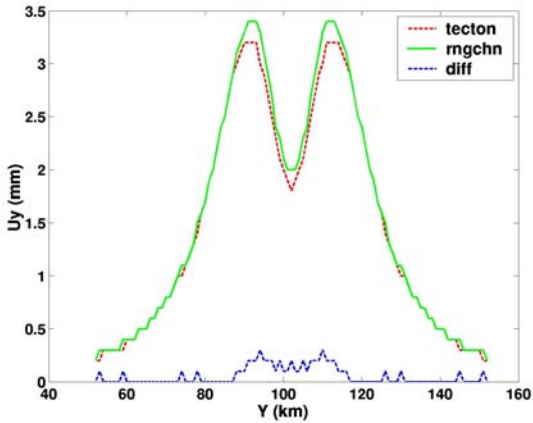


**Figure 8** – Displacement  $U_y$  along a  $X=149.5$  km line for a 18 km deep fault

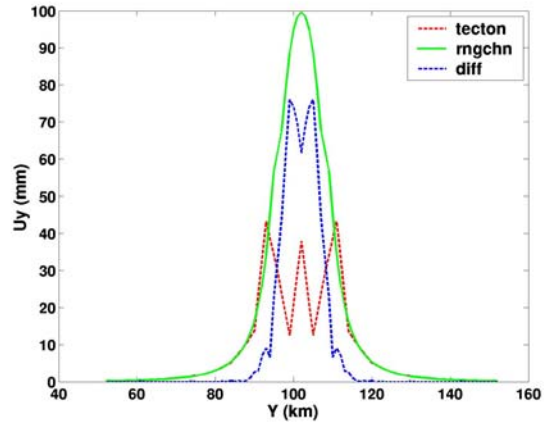


**Figure 9** - Displacement  $U_y$  along a  $X=149.5$  km line for a 10.5 km deep fault

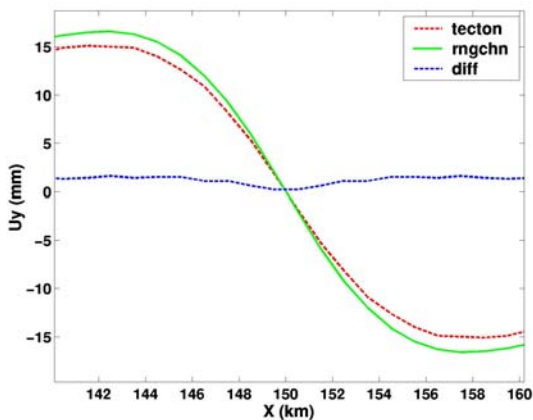


**Figure 10** - Displacement  $U_y$  along a  $Y=102$  km line for a 18 km deep fault

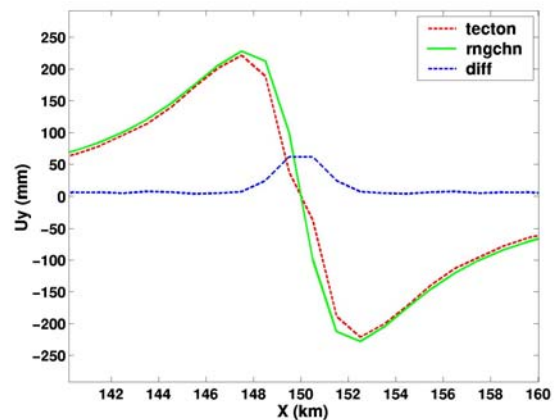


**Figure 11** - Displacement  $U_y$  along a  $Y=102$  km line for a 10.5 km deep fault

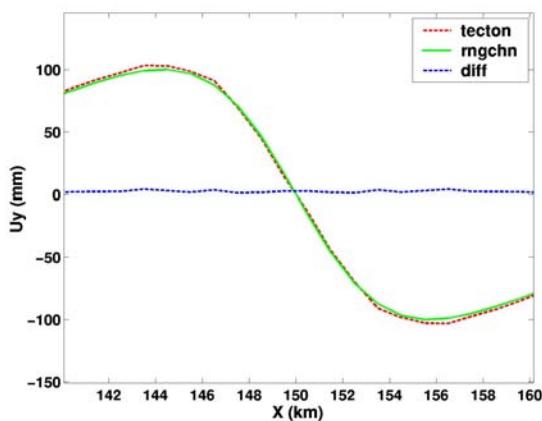


**Figure 12** - Displacement  $U_y$  along a  $Y=90$  km line for a 10.5 km deep fault

## V. Conclusions and perspectives

Despite the fact that our model converges for around 100 000 elements, the boundary conditions still have a significant effect that decreases the overall accuracy of the calculations and the mesh is not enough dense near the fault.

The local convergence would be easily achieved with a little increase in the homothetic ratio to densify the mesh around the fault. To avoid the boundary effects we should increase the Y and Z dimensions of our model. But, with our current mesh density, the resulting model will exceed the maximum capacity of the computer available to us.

A solution would be to use a varying mesh densified in all three directions of space by using the fault as a base. This solution based upon a reasonable number of elements would enable us to suppress the boundary effects. Indeed as our goal is to perform calculations in viscoelastic models a very large model in the elastic case would result in even longer CPU times in the viscoelastic case. We are currently trying to create a model with about 100 000 elements, which should provide accurate results. Such a mesh will allow us to achieve a displacement accuracy of the same order as that measured by GPS or INSAR (typically 1 mm).

## References

- Arnadóttir, T., Jónsson, S., Pedersen, R., Gudmundsson, G. B., 2003. Coulomb stress changes in the South Iceland Seismic Zone due to two large earthquakes in June 2000. *Geophysical Research Letters* 30, 1205, 10.1029/2002GL016495.
- Feigl, K.L., Dupré, E., 1999. RNGCHN : a program to calculate displacement components from dislocations in an elastic half-space with applications for modelling geodetic measurements of crustal deformation. *Computer & Geosciences* 25, 695-704.
- Melosh, H.J., Raefsky, A., 1981. A simple and efficient method for introducing faults into finite element computations. *Bulletin of the Seismological Society of America* 71, 1391-1400.
- Okada, Y., 1985. Surface deformation to shear and tensile faults in a half-space. *Bulletin of the Seismological Society of America* 75 (4), 1135-1154.